Modeling In-Se amorphous alloys

K. Kohary,* V. M. Burlakov, and D. G. Pettifor
Department of Materials, University of Oxford, Parks Road, Oxford OX1 3PH, United Kingdom

D. Nguyen-Manh
UKAEA Culham Division, Culham Science Centre, OX14 3DB, United Kingdom
(Received 20 December 2004; published 26 May 2005)

The structure of amorphous In_xSe_y (a-In_xSe_y) alloys has been studied by a first principles tight-binding molecular dynamics technique. The three-dimensional amorphous structures with different densities at different compositions were prepared by quick quenching from the liquid phase. The characteristics of short-range order, namely radial distribution functions, coordination numbers, bond angle distribution functions, and the electronic structure have been analyzed. The local bonding environments of different In_xSe_y crystals (in particular, In_2Se_3, InSe, and In_4Se_3) were found to be present in the amorphous phase. The average coordination number of indium is mainly four, whereas selenium is mostly two- or threefold coordinated. The majority of the bonds are heteropolar, but homopolar bonds are also present in a-In_xSe_y so that they cannot be excluded from a realistic description of the amorphous structure. Larger content of indium in a-In_xSe_y leads to an increased number of In-In bonds, as expected.

DOI: 10.1103/PhysRevB.71.184203 PACS number(s): 61.43.Bn, 61.43.Dq, 31.15.Ew

I. INTRODUCTION

During the past two decades different compounds of In_xSe_y have been studied extensively for solar cell and ionic battery applications.[1–5] Recently, however, InSe has attracted much attention due to its potential as a high density phase-change data storage medium.[6–9] In phase-change materials the digital information is written or erased in the surrounding crystalline matrix by a heat pulse achieving local amorphization or crystallization of the material. Such type of experiments with InSe were first performed by Nishida *et al.* using a laser pulse.[10] Recently, however, it has been suggested that electron beam sources could be used for amorphization or crystallization in order to create smaller amorphous spot size. The readout process would then also be via the electrons and the actual device is proposed to be a thin film p-n junction.[6–9]

As the amorphous phase of In_xSe_y has the potential for data storage at the nanoscale, it would be helpful to understand its structural and electronic characteristics. Amorphous In_xSe_y (a-In_xSe_y) structures were studied by Burian *et al.* using wide-angle x-ray scattering (WAXS) and extended x-ray absorption fine structure (EXAFS) techniques.[11–13] The goal of these experiments was to study their short-range order through the radial distribution functions. Atomistic modeling of a-$In_{0.5}Se_{0.5}$ was very recently performed by Pena *et al.* using the Car-Parrinello molecular dynamics method.[14] They have concentrated on the chemical ordering present in different amorphous alloys such as a-$In_{0.5}Se_{0.5}$, a-$C_{0.5}Si_{0.5}$, and a-$Si_{0.5}Ge_{0.5}$.

In this paper we study the structural properties of a-In_2Se_3, a-InSe, and a-In_4Se_3. The paper is organized as follows. In the next section we give a brief summary of the structural properties of different crystalline In_xSe_y compounds, which is necessary for understanding the amorphous phase of this material. In Sec. III, we briefly describe the computational method used in our study, and the method of generating our amorphous structures. In Sec. IV, we present the structural properties of a-In_xSe_y materials. In particular, we discuss the properties of short-range order by analyzing the radial distribution functions, average coordination numbers for indium and selenium, the bond angle distribution functions, and the electronic structure for a-InSe. The paper finishes with conclusions in Sec. V.

II. CRYSTALLINE In_xSe_y STRUCTURES

The most studied crystalline compositions of indium-selenide are In_2Se_3, InSe, and In_4Se_3. Among them the most stable compound is In_2Se_3 with the largest melting point ($\sim$1159 K). Other phases such as In_5Se_6 and In_6Se_7 have also been studied experimentally.[15]

Indium-monoselenide (InSe) is considered as a layered semiconductor. The complex layers of InSe are formed by successive atomic planes of Se, In, In, and Se, which are coupled by strong covalent bonds with some weak ionic character. Within the layer the atoms form the conventional zinc-blende structure. The interaction between the complex layers is of Van der Waals type. The structure of three different polytypes (β, γ, and ε) of InSe are very similar, differing only in the stacking order of the layers. In crystalline InSe the coordination number of indium is four, whereas for selenium it is three.[16] Beside heteropolar bonds (between an In and a Se atom) at a distance of 2.64 Å as seen in Table I, there are homopolar bonds between indium atoms: each indium atom has one nearest-neighbor indium atom (at 2.8 Å). There are no Se-Se bonds in this structure.

Crystalline forms of In_2Se_3 can exist in many phases: the layered structure (α phase[17]), the defect wurzite structure (γ phase[18]), and a recently discovered anisotropic structure (κ phase[19,20]). In addition, Ye *et al.* reported a vacancy ordered screw form (VOSF) phase, which exhibits a large op-

TABLE I. Indium-selenium nearest-neighbor crystalline bond lengths and first peak positions of the radial distribution functions in amorphous structures (r_{NN}). Distance to shoulder peak (SP) in a-In_4Se_3 is also given. Amorphous structure data correspond to calculations predicted by DNP basis set. Distances in Å and densities in g/cm^3.

	Crystal				Amorphous		
Composition	Phase	r_{NN}		Density	r_{NN}	SP	Density
In_2Se_3	γ[a]	2.54–2.62[d]	(2.87, 2.96)[e]	5.49	2.63±0.20		5.4
InSe	β[b]	2.64		5.55	2.63±0.19		5.4
In_4Se_3	orthorhombic[c]	2.62–2.80	2.97–3.43	6.02	2.74±0.26	3.1–3.5	6.2

[a]Reference 18.
[b]Reference 16.
[c]Reference 22.
[d]78% of the In-Se bonds.
[e]22% of the In-Se bonds.

tical rotary power.[21] The atomic environment in crystalline In_2Se_3 is very complicated. Atomic bonds in α-In_2Se_3 are at 2.75 and 2.87 Å, whereas γ-In_2Se_3 has In-Se bonds mainly between 2.54 and 2.62 Å, but further nearest-neighbor bonds can be found at 2.87 and 2.96 Å as shown in Table I. Recently, a simplified picture of different In_2Se_3 crystalline structures was given by Ye *et al.*[21] and can be summarized as follows. Both in the α and in the γ polytypes indium has four nearest neighbors. However, in the α phase selenium can have coordination numbers of one, three, and four; in the γ phase selenium is either two- or threefold coordinated. Nevertheless, in both phases the average coordination number of selenium is equal to 2.66.[21] In the VOSF form one third of the cation sites are vacant; if these vacancies are considered as "imaginary" atoms, then the coordination number of each atom would be four. The above simplified picture of Ye *et al.* somewhat contradicts other works. For example, in γ-In_2Se_3 the average coordination number of indium is 4.5 and of selenium is 3.0.[18] Other crystalline In_2Se_3 structures give slightly different results. This discrepancy arises because of the presence of vacancies in these structures, which may lead to even more complicated amorphous structures. There are no nearest-neighbor In-In bonds in In_2Se_3 and Se-Se bonds were only reported in the α phase.[17]

The unit cell of orthorhombic In_4Se_3 contains 28 atoms and it has the most complicated structure among In_2Se_3, InSe, and In_4Se_3. The bonds between the atoms are primarily covalent and the local bonding is similar to that of InSe and In_2Se_3. Nevertheless, the nearest-neighbor environment is very complex. This is illustrated by In-Se bonds having interatomic separations between 2.62 and 2.80 Å (Table I); and In-In bonds at distances of 2.75 and 2.77 Å.[22] There are no Se-Se bonds in this material. Recent theoretical calculations by Bercha *et al.* concentrated on the peculiarities of the band structure, phonon spectrum, and lattice dynamics of crystalline In_4Se_3.[22–24]

III. COMPUTATIONAL METHOD

We have performed first principles tight-binding molecular dynamics simulations to study a-In_2Se_3, a-InSe, and a-In_4Se_3 systems. The three-dimensional amorphous structures in a cubic cell with periodic boundary conditions were prepared by quick quenching from the liquid phase. We calculated the interatomic forces using the *ab initio* program code PLATO (Package for Linear combination of Atomic Type Orbitals).[25,26] One set of structures was prepared using a single numeric (SN) basis set with *s* and *p* orbitals both for indium and selenium. For the other set of structures a double numeric basis set with polarization (DNP) with $sps^*p^*d^*$ orbitals was used. In both cases the orbitals were cutoff at 8.0 a_B ($\approx$4.23 Å). The density functional theory (DFT) calculations were performed within the local density approximation (LDA) and our dynamical simulations use Γ-point sampling for the amorphous phase. We employed the exchange and correlation functional of Goedecker *et al.*[27] and the relativistic pseudopotentials of Hartwigsen *et al.*[28]

It is known that LDA calculations consistently underestimate the value of the band gap of In_xSe_y. For example, Gomes da Costa *et al.* used the "scissor operator" to shift the conduction band of β-InSe.[29] It was also reported that DFT calculations within LDA cannot reproduce the direct to indirect gap transitions as the pressure is increased in γ-InSe and more sophisticated quasiparticle (GW) calculations should be used to overcome this problem.[30] However, the poor description of the conduction states does not effect the ground state properties of a-In_xSe_y, like total energy and forces. We therefore decided to use DFT calculations within the LDA approximation to prepare a-In_xSe_y structures.

In the case of the DNP basis set calculations, the amorphous structures contained 65, 64, and 63 atoms for a-In_2Se_3, a-InSe, and a-In_4Se_3, respectively. Calculations with the SN basis set allow the use of slightly larger unit cells with 125, 124, and 126 atoms, for a-In_2Se_3, a-InSe, and a-In_4Se_3, respectively. In each case we performed simulations with densities of 5.0, 5.4, 5.8, and 6.2 g/cm^3, as the corresponding crystalline densities vary in this range: densities have been reported for InSe around 5.4, 5.8, and 6.0 g/cm^3 and for InSe around 5.5 g/cm^3 (Ref. 17). Crystalline In_4Se_3 has a density close to 6.0 g/cm^3. Furthermore, Burian *et al.* reported that their a-$In_{40}Se_{60}$ sample has a density of 5.0 g/cm^3 (Ref. 13). When modeling the bulk properties of amorphous semiconductor materials, a commonly

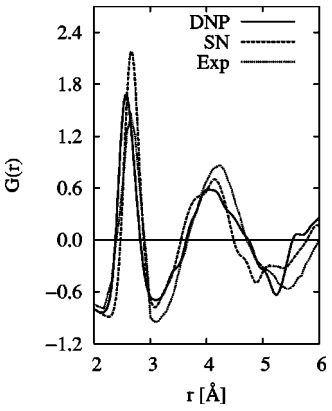

FIG. 1. Reduced radial distribution function of a-In_2Se_3 (ρ=5.0 g/cm^3). Solid and dashed lines show data for structures predicted by DNP and SN basis set simulations, respectively. Dotted line shows measurement from Ref. 13.

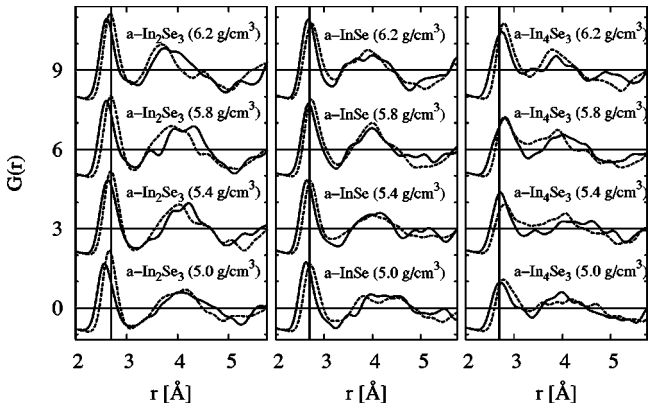

FIG. 2. Reduced radial distribution functions for different a-In_xSe_y structures with different densities. Solid and dashed lines predicted by DNP and SN basis set simulations, respectively. Vertical lines at r=2.7 Å serve as a guide for the eyes.

accepted way to avoid surface effects is to use periodic boundary conditions. Nevertheless, it should be ensured that the simulation cell size is at least three or four times bigger than the cutoff distance of the interaction. In our simulations the smallest simulation cell size was 11.8 Å in comparison with the orbital cutoff (~4.23 Å), which ensures that the choice of periodic boundary conditions has no discernible effect on our results. Each simulation was started from a randomly distributed atomic configuration which was equilibrated at T=4000 K for 1 ps with a 2 fs time step. This is consistent with liquid quench simulations that start from much higher temperatures than the melting temperature in order to generate random models which are independent of their initial states. Then the temperature was reduced to room temperature over 4 ps simulation time with time steps equal to 1 and 2 fs in the case of the DNP basis set; and over 5 ps simulation time with 2.5 fs time step for the structures with the SN basis set calculations. Finally, the conjugate gradient method was used to find the fully relaxed atomic positions for the amorphous structures. These final configurations were used to calculate the pair correlation functions and various structural parameters. For each sample every atom served as a center for the pair correlation function. We have checked that the pair correlation functions obtained in this way are practically the same as the average pair correlation function for the last 100 molecular dynamics configurations at the final stage of the simulation.

IV. AMORPHOUS In_xSe_y STRUCTURES

A. Radial distribution function

The radial distribution function reflects the nature of the short-range order in amorphous materials. In Fig. 1 we show a comparison of the reduced radial distribution function between our computer simulations and experiments for a-In_2Se_3 with a density of ρ=5.0 g/cm^3. The reduced radial distribution is defined by

$$G(r) = 4\pi r(\rho(r) - \rho_0), \tag{1}$$

where $\rho(r)$ is the density of atom centers at a distance r from an atom averaged over the network and ρ_0 is the average density. The predicted positions of the first and second peaks and the width of these peaks are in reasonable agreement with the experimental results of Burian *et al.*,[13] as seen in Fig. 1. The first peak of $G(r)$ is 0.08 Å shifted to the right for the 125-atom structure (SN basis set) compared to the 65-atom structure (DNP basis set). It was shown by Kenny *et al.* that using the PLATO program package DNP basis set calculations are needed to achieve a good accuracy for the structural and cohesive properties for carbon and silicon and the results using the SN (minimal) basis set are rather less good.[25] Therefore, in this paper we focus on the results predicted by the DNP basis set calculations, but we continue to present the results with the SN basis set calculations for comparison. We note here that the minimum to the right of the first peak in Fig. 1 is not as deep within the computer simulations as in the experiment. The origin of this difference might be due to very short quenching times in the simulation compared to those in the experiments, which lead to many liquid-state defects being retained in the amorphous structure. We should take into account this discrepancy in our analysis, but it is still possible to draw some reasonable conclusions about the characteristics of short-range order in a-In_xSe_y.

The reduced radial distribution function for a-In_xSe_y at different densities are shown in Fig. 2. The position of the first peak is between 2.60 to 2.74 Å, which is close to the interatomic distances found in the different crystalline phases (Table I). The general trend is that the position of this first peak shifts to larger distances for the same density but with increasing indium content, and it follows the increase of nearest-neighbor In-Se bonds in the corresponding crystals (Table I). In addition, the same shift can be observed for the same compositions with increasing sample densities, similarly to the case of amorphous carbon.[31] It is also interesting to see whether the changing number of nearest-neighbor homopolar bonds can contribute to the shift of the radial distribution function. This can be illustrated by the partial pair correlation function, which is defined by

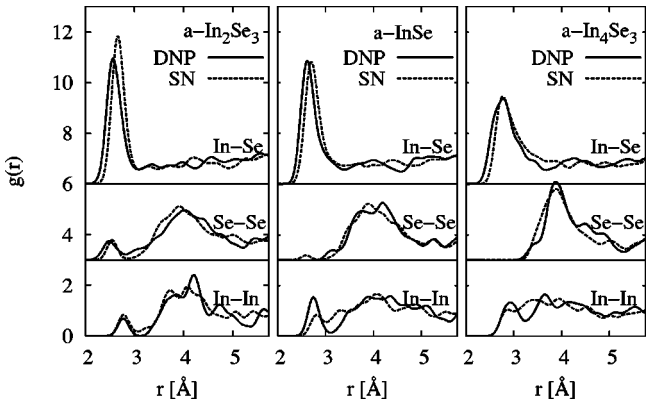

FIG. 3. Partial pair correlation functions in (a) a-In_2Se_3 (ρ=5.0 g/cm^3), (b) a-InSe (ρ=5.4 g/cm^3), and (c) a-In_4Se_3 (ρ=5.8 g/cm^3), for simulations performed by DNP (solid line) and SN basis sets (dashed line).

$$g_{\alpha\beta}(r) = \frac{N}{4\pi r^2 \rho_0 N_\alpha N_\beta} \left\langle \sum_{i\alpha \neq j\beta} \delta(r - r_{i\alpha,j\beta}) \right\rangle, \qquad (2)$$

where N, N_α, and N_β are the total, α type, and β type number of atoms in the simulation cell, respectively, $r_{i\alpha,j\beta}$ is the distance between atoms i (type α) and j (type β), the index $i\alpha$ runs over the α-type atoms, and the angular brackets denote an ensemble average. As expected, the number of nearest-neighbor heteropolar bonds (In-Se) bonds is considerably larger than the number of homopolar bonds, as seen in Fig. 3. The homopolar bonds (In-In and Se-Se) contribute mainly to the left- and right-hand side of the first peak in the radial distribution function, but they do not influence its position. As the majority of the nearest-neighbor bonds are heteropolar, homopolar atomic separations contribute significantly to the second peak of the radial distribution function. The number of nearest-neighbor Se-Se bonds in a-InSe and a-In_4Se_3 structures are negligible, as shown in Figs. 3(b) and 3(c). In a-In_4Se_3 there is a significant contribution of atomic separations between 3.1 and 3.5 Å to the reduced radial distribution function and the border between the first and second peaks is less distinct (Fig. 2). This latter is due to the fact that crystalline In_4Se_3 has In-Se nearest-neighbor interatomic separations of 2.97, 3.16, 3.39, and 3.43 Å as well[22] [apart from the interatomic separations mentioned at the end of Sec. II (see also Table I)], and therefore the corresponding peaks are also expected to be present in the radial distribution function of the amorphous phase.

B. Coordination number

To determine coordination numbers we have taken a cutoff distance for nearest-neighbors as 3.24, 2.97, and 2.7 Å for In-In, In-Se, and Se-Se bonds, respectively. These numbers correspond to a 12.5% increase of the covalent diameters and coincide in a satisfactory way with the second minimum in the radial distribution function. They were first used in the work of Pena *et al.*[14] Our calculations predict that in a-In_xSe_y the average coordination number of indium is close to four, whereas that for selenium is between two and three, as seen in Table II. Both a-InSe and a-In_4Se_3 have homopolar In-In bonds, but Se-Se bonds are absent, which is in accordance with their crystalline forms [see Table II and Figs. 3(b) and 3(c)]. Therefore, the occurrence of Se-Se nearest-neighbor bonds should be considered as defects in these materials. In contrast, a-In_2Se_3 contains both homopolar In-In and Se-Se bonds in the amorphous structure. The number of In-In bonds increases as the indium content increases in a-In_xSe_y, as expected. This increase, however, is not a linear function of indium content: a-In_4Se_3 (57% In) has considerably higher number of In-In bonds than a-In_2Se_3 (40% In) does. On average, every indium atom has approximately 0.5, 1.0, and 1.5 indium nearest neighbor in a-In_2Se_3, a-InSe, and a-In_4Se_3, respectively. This might be crucial for explaining the discrepancies between the transport properties of a-In_xSe_y with different compositions.[32,33]

The coordination numbers predicted in our study seem to be in good agreement with other available data in the literature. The coordination numbers of indium and selenium for a-InSe with 5.4 and 5.8 g/cm^3 density are Z_{In}=3.5 and 3.8; and Z_{Se}=2.7 and 2.9, whereas these data for a-$In_{0.5}Se_{0.5}$ (ρ=5.62 g/cm^3)[14] were claimed to be equal to four and three for indium and selenium, respectively. We have also found a reasonable agreement between our a-In_2Se_3 (ρ=5.0 g/cm^3) and experimental data: the partial coordination numbers $Z_{In\text{-}In}$, $Z_{In\text{-}Se}$, and $Z_{Se\text{-}Se}$ are predicted to be equal to 0.2, 3.1, and 0.4, whereas the multi-shell fit of Burian *et al.* found $Z_{In\text{-}In}=0.55\pm0.5$, $Z_{In\text{-}Se}=3.0\pm0.5$, and $Z_{Se\text{-}Se}=0.55\pm0.5$. Furthermore, both in the experiments and in our study the coordination number for indium is predicted to be around four. However, the coordination number for selenium was found to be three in the experiments compared with our value of Z_{Se}=2.4. In our a-In_2Se_3 structures coordination numbers of selenium are close 2.66, which is the corresponding coordination number in the crystal according to the simplified picture of Ye *et al.*[21] The discrepancy between the prediction of theory and experiments might be attributed to the different approaches determining coordination numbers: cutoff in our case and multishell fitting in the experiments.

We found considerable fluctuations in coordination numbers in a-In_xSe_y, as seen in Table III. The coordination number for indium is mainly four, but there are also indium atoms with threefold and fivefold coordination, apart from a small number of indium atoms having coordination numbers less than three. Selenium is mainly two- or threefold coordinated, with some exceptions of fourfold coordination. Therefore, our study suggests that a-In_xSe_y cannot be considered as a classical random network material,[34] as the local topology is not the same as in the the corresponding crystal due to the fluctuations in coordination numbers.

Our analysis of the structural data revealed that some indium atoms are isolated with a coordination number equal to zero. An analysis of the PLATO bond order and bond energy values for our a-In_xSe_y structures has shown that the above cutoff criteria for nearest-neighbor bonds may be too simplistic. For example, there are some cases where atoms show strong bonding behavior despite being separated at a distance further than the above mentioned cutoff distance; and also there are cases where we found the opposite. Nevertheless, the number of such type of irregularities is small and there-

TABLE II. Average and partial coordination numbers for In and Se for different compositions and densities (ρ in g/cm^3). Data correspond to structures predicted by DNP basis set simulations.

	ρ	Z_{In}	$Z_{In\text{-}In}$	$Z_{In\text{-}Se}$	Z_{Se}	$Z_{Se\text{-}In}$	$Z_{Se\text{-}Se}$
	5.0	3.3	0.2	3.1	2.4	2.1	0.4
a-In_2Se_3	5.4	4.1	0.5	3.6	2.7	2.4	0.3
	5.8	4.0	0.2	3.8	2.7	2.5	0.2
	6.2	4.1	0.3	3.8	2.8	2.5	0.3
a-$In_{40}Se_{60}$[d]	5.0	4.0	0.55±0.5	3.0±0.5	3.0	NR[f]	0.55±0.5
γ-In_2Se_3[a]	5.49	4.5	0.0	4.5	3.0	3.0	0.0
In_2Se_3[e]		4.0	0.0	4.0	2.66	2.66	0.0
	5.0	3.4	0.8	2.6	2.6	2.6	0.0
a-InSe	5.4	3.5	0.8	2.7	2.7	2.7	0.0
	5.8	3.8	0.9	2.8	2.9	2.8	0.1
	6.2	3.9	0.9	3.1	3.1	3.1	0.0
β-InSe[b]	5.55	4.0	1.0	3.0	3.0	3.0	0.0
	5.0	2.5	0.6	2.0	2.6	2.6	0.0
a-In_4Se_3	5.4	3.5	1.5	2.0	2.6	2.6	0.0
	5.8	3.3	1.2	2.1	2.8	2.8	0.0
	6.2	4.0	1.8	2.2	3.0	3.0	0.0
In_4Se_3[c]	6.02	3.0	1.0	2.0	2.7	2.7	0.0

[a]Reference 18.
[b]Reference 16.
[c]Reference 22.
[d]Reference 13.
[e]Reference 21.
[f]Not reported.

fore, we have continued to use the experimental criteria for the cutoff when determining the number of nearest-neighbor bonds.

C. Bond angle distribution function

The detailed modeling of the atomic structure also allows the study of the bond angle distribution function and the ring statistics (shortest closed path through nearest-neighbor atoms with each bond passed only once[35]) for every amorphous structure. Figure 4(a) illustrates the bond angle distribution function of *a*-In_2Se_3 (ρ=5.0 g/cm^3). The maximum of the main peak is around 100° and there is the sign of a "shoulder" peak at around 109° corresponding to tetrahedral bonding. Both tails of the distribution are very pronounced and large bond angles can also be found in the amorphous

TABLE III. Percentage of In and Se atoms with different coordination numbers for different compositions and densities (ρ in g/cm^3). Data correspond to structures predicted by DNP basis set simulations.

	ρ	$Z_{In}=1$	$Z_{In}=2$	$Z_{In}=3$	$Z_{In}=4$	$Z_{In}=5$	$Z_{Se}=2$	$Z_{Se}=3$	$Z_{Se}=4$
	5.0	11.5	0.0	19.2	65.4	0.0	59.0	41.0	0.0
a-In_2Se_3	5.4	0.0	3.8	3.8	73.1	15.4	33.3	56.4	7.7
	5.8	0.0	0.0	15.4	73.1	11.5	38.5	53.8	7.7
	6.2	0.0	0.0	19.2	57.7	19.2	25.6	59.0	12.8
	5.0	6.2	9.4	15.6	62.5	3.1	43.8	50.0	6.2
a-InSe	5.4	3.1	9.4	6.2	62.5	12.5	37.5	53.1	9.4
	5.8	0.0	6.2	21.9	62.5	9.4	28.1	50.0	21.9
	6.2	9.4	6.2	3.1	43.8	37.5	12.5	71.9	12.5
	5.0	13.9	30.6	16.7	25.0	5.6	37.0	51.9	7.4
a-In_4Se_3	5.4	8.3	5.6	30.6	41.7	13.9	44.4	48.1	7.4
	5.8	8.3	13.9	25.0	41.7	11.1	29.6	63.0	3.7
	6.2	0.0	2.8	33.3	38.9	13.9	22.2	37.0	33.3

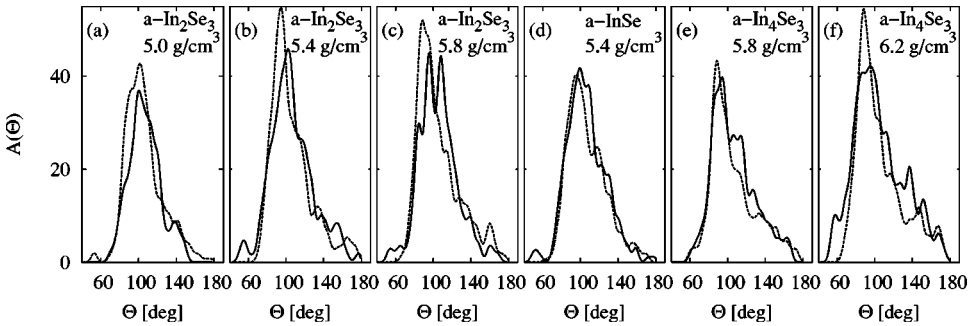

FIG. 4. Bond angle distribution functions of different a-In_xSe_y structures. Solid and dashed lines show data corresponding to structures predicted by DNP and SN basis set simulations, respectively.

phase. As seen in Fig. 4(a), the majority of the bond angles are in the interval between 80° and 130°. The bond angle distribution function in a-In_2Se_3 is very similar for all different densities [Figs. 4(a)–4(c)]. In addition, it has almost the same shape in a-InSe [Fig. 4(d)] and in a-In_4Se_3 [Figs. 4(e) and 4(f)]. Crystalline InSe has bond angles equal to 98.4° (In-Se-In and Se-In-Se) and 119° (In-In-Se). In crystalline In_4Se_3 there are bond angles of 100.6°, 101.9°, 108.4°, and 157.9°. These local configurations can be found in any a-In_xSe_y independently of its composition, as seen in Fig. 4. We found that in a-In_xSe_y there is only a minor contribution from fragments which have two or three nearest-neighbor selenium atoms. In a-In_2Se_3 the occurrence of In-In-In fragments is also negligible.

Crystalline InSe and InSe contain six-member rings, but in In_4Se_3 five-member rings are also present. In our molecular dynamics simulations we have found that the majority of rings belong to these groups, but at the same time four-, seven- and eight-member rings can also be found in the amorphous structures. However, our ring statistics do not possess any specific characteristics due to the small number of atoms in the unit cell and the large number of coordination defects we found in a-In_xSe_y. Larger unit cells will be needed for gaining a reliable ring statistics of a-In_xSe_y.

D. Electronic structure

Amorphous In_xSe_y films, as well as their crystalline counterparts, are semiconductors with a gap larger than 1 eV. We have calculated the electronic density of states (DOS) of a-InSe at different densities as shown in Fig. 5. The DOS of crystalline β-InSe with a calculated gap of 0.5 eV is also plotted for comparison. The shape of the DOS for a-InSe with different densities show similarities to the crystalline DOS, but they display a pseudogap with a finite DOS at the Fermi energy in contrast with experimental data. This is due to the liquid quench simulations, which introduce considerably more defects than observed experimentally, thereby leading to a large number of localized states inside the real gap.

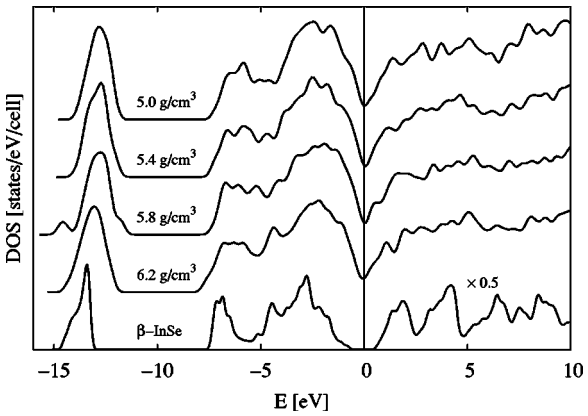

FIG. 5. Electronic density of states (DOS) of a-InSe with different densities compared to crystalline β-InSe. Perpendicular line at zero indicates Fermi energy.

V. CONCLUSION

This paper reports an atomistic study of the short-range order in a-In_xSe_y with different compositions. The local bonding environments of different InSe crystals (In_2Se_3, InSe, and In_4Se_3) were found to be present in the amorphous phase. The radial distribution function of our a-In_2Se_3 sample with $\rho = 5.0\ g/cm^3$ agrees reasonably well with experiment. We have found that the average coordination number for indium is mainly four, whereas selenium is mainly two- or threefold coordinated. Our calculations suggest that a-In_xSe_y cannot be considered as a classical random network material, as we have found significant fluctuations in coordination numbers. In a-In_xSe_y the majority of nearest neighbors are heteropolar In-Se bonds, but there are also some homopolar bonds. In accordance with their crystalline form in a-InSe and a-In_4Se_3 homopolar In-In bonds exist, whereas Se-Se bonds are absent. In contrast, a-In_2Se_3 has both In-In and Se-Se bonds. The number of In-In bonds increases by increasing the indium content in a-In_xSe_y, as expected. This might be crucial for explaining the discrepancies between the transport properties of a-In_xSe_y with different compositions.

ACKNOWLEDGMENTS

This research was funded by Hewlett-Packard Laboratories (Palo Alto, California). We acknowledge interesting and valuable discussions with Jim Brug, C. C. Yang, Gary Gibson, Chris Nauka, Alison Chaiken, and Jacek Jasinski. K.K. and D.N.M. would also like to thank Andrew Horsfield and Steve Kenny for helpful discussions regarding PLATO. The calculations were performed using the computer facilities of the Materials Modeling Laboratory and of the Oxford Supercomputer Centre (University of Oxford).

*Electronic address: krisztian.kohary@materials.ox.ac.uk

[1] J. P. Guesdon, B. Kobbi, C. Julien, and M. Balkanski, Phys. Status Solidi A **102**, 327 (1987).
[2] J. F. Sanchez-Royo, A. Segura, O. Lang, E. Schaar, C. Pettenkofer, R. Roa, and A. Chevy, J. Appl. Phys. **90**, 2818 (2001).
[3] C. Julien, I. Samaras, M. Tsakiri, P. Dzwonkowski, and M. Balkanski, Mater. Sci. Eng., B **3**, 25 (1989).
[4] V. K. Lukyanyuk, M. V. Tovarnitskii, and Z. D. Kovalyuk, Phys. Status Solidi A **104**, K41 (1987).
[5] D. Fargues, G. Tyuliev, G. Brojerdi, M. Eddrief, and M. Balkanski, Surf. Sci. **370**, 201 (1997).
[6] G. A. Gibson, A. Chaiken, K. Nauka, C. C. Yang, R. Davidson, A. Holden, R. Bicknell, B. S. Yeh, J. Chen, H. Liao, S. Subramanian, D. Schut, J. Jasinski, and Z. Liliental-Weber, Appl. Phys. Lett. **86**, 051902 (2005).
[7] A. Chaiken, G. Gibson, J. Chen, B. Yeh, J. Jasinski, Z. Liliental-Weber, K. Nauka, C. Yang, D. Linding, and S. Subramanian (unpublished).
[8] A. Chaiken, G. A. Gibson, K. Nauka, C. C. Yang, B. S. Yeh, R. Bicknell-Tassuis, J. Chen, J. Jasinski, Z. Liliental-Weber, and D. D. Lindig, "Reversible Optical Recording on Epitaxial Indium Selenide Phase-Change Media," paper HH.1.9, 2003 MRS Fall Meeting, Boston, MA, 2003 (unpublished).
[9] G. A. Gibson, A. Chaiken, K. Nauka, C. C. Yang, R. Davidson, A. Holden, D. D. Lindig, R. Bicknell-Tassuis, J. Chen, H. Liao, D. Neiman, D. Schut, S. Subramanian, B. S. Yeh, J. Jasinski, and Z. Liliental-Weber, "An Electron-Beam Addressed Phase-Change Recording Medium," paper HH.2.6, 2003 MRS Fall Meeting, Boston, MA, 2003 (unpublished).
[10] T. Nishida, M. Terao, Y. Miyauchi, S. Horigome, T. Kaku, and N. Ohta, Appl. Phys. Lett. **50**, 667 (1987).
[11] A. Jablonska, A. Burian, A. M. Burian, J. Szade, O. Proux, J. L. Hazemann, A. Mosset, and D. Raoux, J. Non-Cryst. Solids **299-302**, 238 (2002).
[12] A. Jablonska, A. Burian, A. M. Burian, P. Lecante, and A. Mosset, J. Alloys Compd. **328**, 214 (2001).
[13] A. Burian, A. M. Burian, J. Weszka, M. Zelechower, and P. Lecante, J. Mater. Sci. **35**, 3121 (2000).
[14] E. Y. Pena, M. Mejia, J. A. Reyes, R. M. Valladares, F. Alvarez, and A. A. Valladares, J. Non-Cryst. Solids **338-340**, 258 (2004).
[15] K. Imai, K. Suzuki, T. Haga, Y. Hasegawa, and Y. Abe, J. Cryst. Growth **54**, 501 (1981).
[16] S. Nagel, A. Baldereschi, and K. Maschke, J. Phys. C **12**, 1625 (1979).
[17] S. Popovic, A. Tonejc, B. Grzeta-Plenkovic, B. Celustka, and R. Trojko, J. Appl. Crystallogr. **12**, 416 (1979).
[18] A. Likoforman, D. Carre, and R. Hillel, Acta Crystallogr., Sect. B: Struct. Crystallogr. Cryst. Chem. **34**, 1 (1978).
[19] C. H. de Groot and J. Moodera, J. Appl. Phys. **89**, 4336 (2001).
[20] J. Jasinski, W. Swider, J. Washburn, Z. Liliental-Weber, A. Chaiken, K. Nauka, G. A. Gibson, and C. C. Yang, Appl. Phys. Lett. **81**, 4356 (2002).
[21] J. Ye, S. Soeda, Y. Nakamura, and O. Nittono, Jpn. J. Appl. Phys., Part 1 **37**, 4264 (1998).
[22] D. M. Bercha, K. Z. Rushchanskii, and M. Sznajder, Phys. Status Solidi B **212**, 247 (1999).
[23] D. M. Bercha, K. Z. Rushchanskii, L. Y. Kharkhalis, and M. Sznajder, Condens. Matter Phys. **3**, 749 (2000).
[24] D. M. Bercha, L. Y. Kharkhalis, A. I. Bercha, and M. Sznajder, Phys. Status Solidi B **203**, 427 (1997).
[25] S. D. Kenny, A. P. Horsfield, and H. Fujitani, Phys. Rev. B **62**, 4899 (2000).
[26] A. P. Horsfield, Phys. Rev. B **56**, 6594 (1997).
[27] S. Goedecker, M. Teter, and J. Hutter, Phys. Rev. B **54**, 1703 (1996).
[28] C. Hartwigsen, S. Goedecker, and J. Hutter, Phys. Rev. B **58**, 3641 (1998).
[29] P. Gomes da Costa, R. G. Dandrea, R. F. Wallis, and M. Balkanski, Phys. Rev. B **48**, 14135 (1993).
[30] G. Ferlat, H. Xu, V. Timoshevskii, and X. Blase, Phys. Rev. B **66**, 085210 (2002).
[31] N. A. Marks, N. C. Cooper, D. R. McKenzie, D. G. McCulloch, P. Bath, and S. P. Russo, Phys. Rev. B **65**, 075411 (2002).
[32] S. Marsillac, J. C. Bernede, and A. Conan, J. Mater. Sci. **31**, 581 (1996).
[33] A. Chaiken, K. Nauka, G. A. Gibson, H. Lee, and C. C. Yang, J. Appl. Phys. **94**, 2390 (2003).
[34] P. K. Gupta, J. Non-Cryst. Solids **195**, 158 (1996).
[35] D. S. Franzblau, Phys. Rev. B **44**, 4925 (1991).